Korean J. Chem. Eng., 35(7), 1556-1569 (2018)
DOI: 10.1007/s11814-017-0326-4

pISSN: 0256-1115
eISSN: 1975-7220

Toward an intelligent approach for predicting surface tension of binary mixtures containing ionic liquids

Reza Soleimani*, Amir Hossein Saeedi Dehaghani,†, Navid Alavi Shoushtari***, Pedram Yaghoubi****, and Alireza Bahadori*****

*Young Researchers and Elite Club, Neyshabur Branch, Islamic Azad University, Neyshabur, Iran
**Department of Petroleum Engineering, Faculty of Chemical Engineering, Tarbiat Modares University, Tehran 14115-143, Iran
***210 15 Ave SE, Calgary, Alberta, Canada T2G 0B5
****Department of Physics, University of Kashan, Kashan, Iran
*****School of Environment, Science and Engineering, Southern Cross University, Lismore, New South Wales 2480, Australia
(*Received 13 June 2017 • accepted 22 November 2017*)

Abstract−Knowledge of the surface tension of ionic liquids (ILs) and their related mixtures is of central importance and enables engineers to efficiently design new processes dealing with these fluids on an industrial scale. It's obvious that experimental determination of surface tension of every conceivable IL and its mixture with other compounds would be a herculean task. Besides, experimental measurements are intrinsically laborious and expensive; therefore, accurate prediction of the property using a reliable technique would be overwhelmingly favorable. To do so, a modeling method based on artificial neural network (ANN) trained by Bayesian regulation back propagation training algorithm (trainbr) has been proposed to predict surface tension of the binary ILs mixtures. A total set of 748 data points of binary surface tension of IL systems within temperature range of 283.1-348.15 K was used to train and test the applied network. The obtained results indicated that the predictive values and experimental data are quite matching, representing reliability of the used ANN model for such purpose. Also, compared with other methods, such as SVM, GA-SVM, GA-LSSVM, CSA-LSSVM, GMDH-PNN and ANN trained with trainlm algorithm the proposed model was better in terms of accuracy.

Keywords: Ionic Liquids, Surface Tension, Binary Mixtures, Prediction, Artificial Neural Network

INTRODUCTION

Ionic liquids (ILs), as a new family of ionic organic salts having melting points near or below room temperature, are typically made up of relatively large organic cations and small inorganic or organic anion. The relatively low melting point of ILs results from their high degree of asymmetry, which puts obstacles in the way of ILs to form crystals. ILs have recently attracted great attention of both academia and industry by virtue of their tempting features in competition with other traditional compounds for different applications, such as extremely low volatility, high thermal and electronic stability, high ionic conductivity, a wide liquid temperature and good solubility [90]. However, the most salient feature of ILs is that their properties can be finely adjusted to fulfill the requirements of any particular application by changing the cations and anions. This is why they can legitimately be christened "designable materials" [23,30,59]. Definitely, for accomplishment of efficient process design knowledge about thermophysical, physicochemical, and/or thermodynamic properties of the involved ILs and their related mixtures is of considerable importance [28]. For designing and operation of new industrial processes such as absorption, extraction and distillation involving ILs, the accurate knowledge of surface tension of such fluids and their relevant mixtures is necessary [11,66].

It is obvious that the properties of every conceivable IL and its mixture with other compounds (Note that industrial processes are mostly concerned with mixtures of two or more components) cannot be obtained solely by experimental measurement since there are limitless numbers of possible systems. Besides, experimental measurements are intrinsically time-consuming, costly, and with probable non-negligible uncertainties [28]. So, it is highly desirable to develop and utilize predictive methods for estimating the various properties of these kinds of systems.

Rigorous reviews on the methods for prediction of surface tension of pure compounds have been already well presented in the literature [27-29,68]. In addition, Tariq et al. [83] and Gharagheizi et al. [30] conducted reviews about various methods used especially for the prediction of the surface tension of ILs and we do not repeat them here. However, there are two main conclusions to be drawn from the aforementioned literature reviews:

- Surface tension of ILs is estimated by a few models, so modeling of such property of ILs is still an open field of research.
- Gharagheizi et al. [30] stated that these methods, the ones used

†To whom correspondence should be addressed.
E-mail: asaeedi@modares.ac.ir

for modeling of surface tension of ILs, have their own disadvantages. They mentioned associated shortcomings.

In addition, group contribution method, which was used by Gharagheizi et al. [30], demands thorough understanding of the structure of the ILs and, in some cases, are not beneficial in time and simplicity, and above all the group parameters of various functional groups in the IL structures are not yet specified, so such methods are still very restricted in their usage [39]. Thus, there is a need for alternative methods.

The artificial intelligence methods such as artificial neural networks (ANNs), evolutionary computation (EC), and fuzzy systems (FS), which allows developing a model for the complicated systems, have recently appeared as capable approaches. ANNs have been the focus of much attention during the past decades as viable and efficient tools in numerous research areas due to their simplicity and multi-functionality [40]. Basically, ANNs are numerical configurations emerging from the learning process in the human brain [74]. The advantages of artificial neural networks can generally be perceived as their capability to map any relation with any degree of complexity and self-learning ability which eliminates the need for reprogramming [40]. Further and detailed explanations about ANN are available in the literature [16,96].

This well-known sort of artificial intelligence paradigm has been successfully applied to analyze different properties, e.g., ANNs have been used for prediction of the thermal conductivity of pure gases at atmospheric pressure over a broad range of temperatur [19], to assess the conductivities of binary gaseous mixtures at atmospheric pressure [20], to predict the surface tension, viscosity, and thermal conductivity for common organic solvents [42], and characterize the basic properties of pure substances and petroleum fractions [10]. In addition ANN approaches have been applied to predict metal alloys properties [5,65,67,82]. Also, a comprehensive review has been carried out by Taskinen and Yliruusi [84] about works on neural network anticipation of physicochemical properties from a pharmaceutical research point of view such as boiling point, heat capacity, critical pressure, vapor pressure, critical temperature, enthalpy of sublimation, surface tension, density, viscosity, thermal conductivity, acentric factor and heat of vaporization.

In addition, Urata et al. [88], He et al. [36], Mohanty [62], Rohani et al. [72], Lashkarbolooki et al. [48,49] have applied ANN to model and predict phase equilibria of different systems. Laugier and Richon [52] used neural network system as a prediction tool for the PVT behavior of refrigerants. Mohebbi et al. [63] used the ANN model to predict the liquid density of 19 pure components and six mixtures of refrigerants. Furthermore, Lashkarbolooki et al. [50] compared the sufficiency of the ANN model with EOS's for prediction of solid solubility in supercritical carbon dioxide.

More importantly, success stories of ANN for correlating the properties of the ILs have already been reported by several groups around the world. Zeinolabedini Hezave and coworkers demonstrated the good capability of ANNs to predict thermal conductivity of pure ILs [40], the binary heat capacity [47], ternary electrical conductivity [39], ternary bubble points [38], binary density [48], and ternary viscosity [45] of the systems containing ILs. Lazzús [53] reported successful application of ANN for a total of 2410 data sets in predicting density within a wide range of temperatures and pressures (ρ-T-P), corresponding to 250 ionic liquids. In addition, Torrecilla et al. [86] presented an optimized ANN model to estimate the melting point of a group of 97 imidazolium salts of diverse anions. Their model was able to correlate the melting point with mean prediction error of 1.30%, a regression coefficient of 0.99 and a mean P-value of 0.92. Bini and coworkers [9] reported that the recursive neural network (RNN) was an applicable tool to predict the melting points of several pyridinium based ILs. Miao et al. [60] used the ANN model to predict the compositional viscosity of binary mixtures of room temperature ILs [C_n-mim] [NTf2] with n=4, 6, 8, 10 in methanol and ethanol for the whole domain of molar fraction within an extensive temperature (T=293.0-328.0 K) range. Eslamimanesh et al. [18] applied ANN procedure to represent the solubility of supercritical CO_2 in 24 mostly used ionic liquids. Note that employed pseudo-critical properties of ionic liquids in their studies, were estimated by group contribution method. Torrecilla et al. [86] explored, in addition to multiple linear regression (MLR) and multiple quadratic regression (MQR), radial basis network (RB), and multiLayer perceptron (MLP) neural network models predict the CO_2 solubility in 1-n-ethyl-3-methylimidazolium hexafluorophosphate, 1-n-hexyl-3-methylimidazolium hexafluorophosphate, 1-n-butyl-3-methylimidazolium tetrafluoroborate, 1-n-hexyl-3-methylimidazolium tetrafluoroborate and 1-n-octyl-3-methylimidazolium tetrafluoroborate ILs at sub and supercritical conditions. Safamirzaei and Modarress [77] proposed a scheme based on neural network paradigm and molecular properties to model solubility of carbon dioxide, carbon monoxide, argon, oxygen, nitrogen, methane and ethane in 1-butyl-3-methylimidazolium tetrafluoroborate and also they [76] used ANN for prediction of Henry's law constants of gases in [bmim][PF6] at low values of pressure. Interested readers are referred to the literature for more application of ANN and other machine learning algorithms such as support vector machine (SVM), decision tree (DT) algorithm and gene expression programming (GEP) in the field of ILs [1,2,15,21,32,61,64,78,80,81,86].

To pursue the research in computational intelligence schemes and combine them with ILs, in this study ANN with two hidden layer and trained by trainbr algorithm was applied to anticipate the surface tension of binary mixtures containing ILs. Reviewing the literature indicates a few papers are devoted solely to the topic of predicting surface tension of mixtures, especially multicomponent system containing ILs [6,34,37,46,66].

DATASET PREPARATION

The experimental data employed for modeling consisted of 748 binary surface tension (ST) data points at atmospheric pressure were assembled from the NIST Standard Reference Database [3,17,26,41,43,70,71,91-94]. The selection of input variables as the model's independent variables was the subsequent step after identifying and assembling the data set. In this regard, the operational temperature (T), the IL component compositions (x_{IL}), molecular weight of IL components (Mw_{IL}) and density of IL components (ρ_{IL}) along with the boiling point ($Tb_{non\text{-}IL}$) and molecular weight ($Mw_{non\text{-}IL}$) of non-IL component were introduced as entrance parameters. Table 1 has been provided to illustrate Mw_{IL} and ρ_{IL}; in addition, the $Tb_{non\text{-}IL}$ and

Table 1. Molecular weight and specific density range of used ILs in this study [34]

No.	Name	Formula	Mw gr·mol^{-1}	Specific density/ Kg·m^{-3} (In the range of investigated temperature)	Maximum experimental error margin (specific density)	Ref.
1	1-Hexyl-3-methylimidazolium bis[(trifluoromethyl)sulfonyl]imide ([HMIM] [TF2N])	C12H19F6N3O4S2	447.42	1324-1385.4 @ (283.1-348.15) K	±4	[3]
2	1-Butyl-3-methylimidazolium bis[(trifluoromethyl)sulfonyl]imide ([BMIM] [TF2N])	C10H15F6N3O4S2	419.36	1419.8-1438.9 @ (293.15-313.15) K	±1.6	[87]
				1436 @ (298) K	±15	[91]
3	1-Ethyl-3-methylimidazolium bis[(trifluoromethyl)sulfonyl]imide ([EMIM][TF2N])	C8H11F6N3O4S2	391.31	1503.3-1523.6 @ (293.15-313.15) K	±2.7	[79]
4	1-Butyl-3-methylimidazolium L-lactate ([BMIM][L-lactate])	C11H20N2O3	228.29	1097.7-1111.2 @ (298.15-318.15) K	±6	[41]
5	1-Butyl-3-methylimidazolium tetrafluoroborate ([BMIM] [BF_4])	C8H15BF4N2	226.02	1200.85 @ 298.15 K	±0.4	[89]
6	1-Ethyl-3-methylimidazolium tetrafluoroborate ([EMIM] [BF_4])	C6H11BF4N2	197.97	1280.5 @ 298.15 K	±1.9	[79]
7	1-Hexyl-3-methylimidazolium tetrafluoroborate ([HMIM] [BF_4])	C10H19BF4N2	254.08	1145.6 @ 298.15 K	±1.1	[44]
8	1-Methyl-3-octylimidazolium tetrafluoroborate ([OMIM] [BF_4])	C12H23BF4N2	282.13	1103.7 @ 298.15 K	±2.9	[33]
9	1-Ethyl-3-methylimidazolium butyl sulfate ([EMIM][BS])	C10H20N2O4S	264.34	1176.2 @ 298.15 K	±1.2	[12]
10	1-Ethyl-3-methyl imidazolium octyl sulfate ([EMIM] [OS])	C14H28N2O4S	320.45	1095.7 @ 298.15 K	±1	[12]
11	1-Ethyl-3-methyl imidazolium-hexyl sulfate ([EMIM] [HS])	C12H24N2O4S	292.39	1130.4 @ 298.15 K	±1.4	[24]
12	1-Ethyl-3-methyl imidazolium-ethyl sulfate ([EMIM] [ES])	C8H16N2O4S	236.29	1237.2 @ 298.15 K	±0.4	[25]
13	1-Ethyl-3-methyl imidazolium methyl sulfate ([EMIM][MS])	C7H14N2O4S	222.26	1289.48 @ 293.15 K	±0.53	[12]
14	3-Ethyl-1-methylimidazolium (S)-2-hydroxypropanoate ([EMIM][L-lactate])	C9H16N2O3	200.23	1146.1 @ 298.15 K	±2.8	[55]
15	3-Butyl-1-methyl-1H-imidazolium (S)-2-amino-4-carboxybutanoate ([BMIM][Glu])	C13H23N3O4	285.34	1175.2-1192.4 @ 308.15- 343.15 K	±2.8	[94]

Table 2. Molecular weight and boiling point of investigated non-IL components [34,54]

No.	Name	Formula	Mw/gr·mol^{-1}	Boiling point/K
1	1-Octene	C_8H_{16}	112.21	395±2
2	Dimethyl Sulfoxide	$C_2H_6O_S$	78.13	464±7
3	Acetonitrile	C_2H_3N	41.05	354.8±0.4
4	Tetrahydrofuran	C_4H_8O	72.11	339±1
5	Methanol	CH_4O	32.04	337.8±0.3
6	Water	H_2O	18.02	373.17±0.04
7	1-Butanol	$C_4H_{10}O$	74.12	390.6±0.8
8	Ethanol	C_2H_6O	46.07	351.5±0.2
9	1-Propanol	C_3H_8O	60.1	370.3±0.5

$Mw_{non\text{-}IL}$ are illustrated in Table 2 [3,12,24,25,33,41,44,54,55,79,87,89,91,94]. So, the functionality of binary surface tension of ILs is given as follows:

$$\sigma = f(T, x_{IL}, Mw_{IL}, \rho_{IL}, Tb_{non\text{-}IL}, Mw_{non\text{-}IL})$$

Note that the model needs some criteria to distinguish the sub-

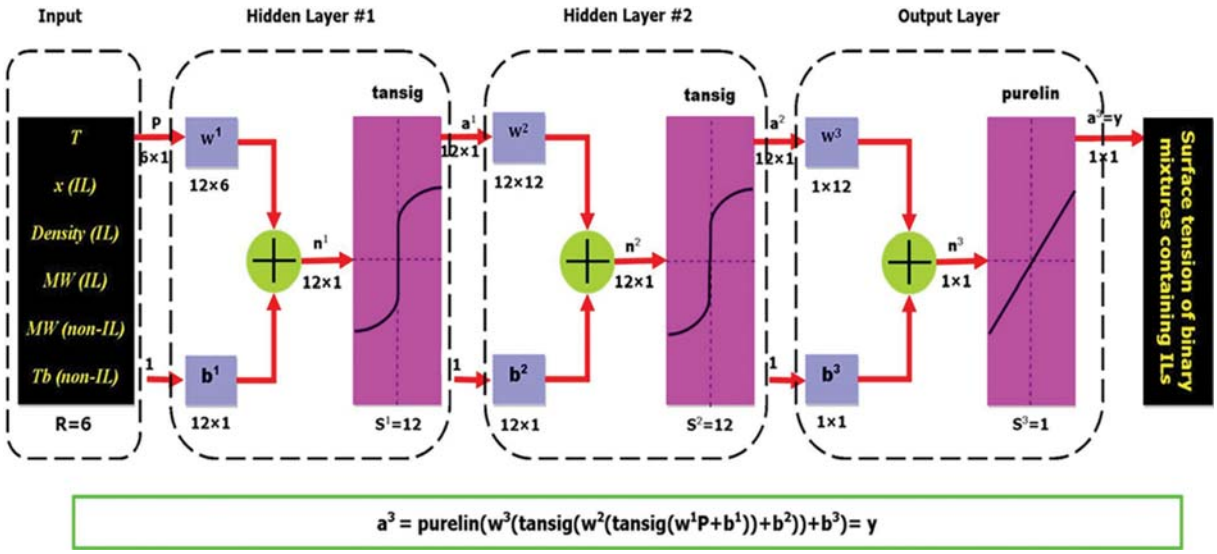

Fig. 1. ANN structure designed for prediction of the surface tension of binary mixtures.

stances involved. For this purpose, molecular weight, density and boiling point were considered as the parameters to differentiate among the different substances. Also, there are different operational parameters including pressure, temperature and different compositions which affect directly the output value (i.e., surface tension). Herein the considered parameters are the composition and temperature at constant pressure (atmospheric pressure), which leads to have different conditions [38,40,45].

ARTIFICIAL NEURAL NETWORK

Artificial neural network (ANN) combines artificial neurons which are computational models inspired in the natural neurons, to obtain patterns and discern trends that are extremely complex.

There are several types of ANNs and the most common type of ANN is the multi-layer feed-forward neural network, which consists of groups of interconnected neurons divided into three sets: input layer, hidden layer and output layer, where each layer is made up of a set of neurons that partake of the same input and output connections, but do not connect amongst themselves. Also, the connections strictly travel in one itinerary (input to output) and there is no feedback (loops). The neurons in the input layer accept real world inputs from an external source, and the neurons in the output layer transmit the dependent variables.

The task of determining the number of neurons in the input and output layers, hence, is specified by the input and output variables, respectively. In between the input and the output layer(s) there is a hidden layer (there may be several hidden layers) that can have any number of neurons. There were no definite values for the numbers of hidden layers and the neurons comprising this/these layer(s), unlike the output and input neurons. So there is no rule of thumb to find how many you need as it depends on the intricacy of the issue being solved by the network and in demand accuracy.

The outputs of hidden and the output neurons are computed by transforming their inputs by dint of a transfer function. So transfer function commutes a neuron's weighted sum of all inputs to its output activation.

The three transfer functions, named Linear transfer function (purelin), Log-Sigmoid transfer function (logsig) and Hyperbolic Tangent Sigmoid (tansig), are the most-used transfer functions and are formulated as follows:

- purelin

$$\varphi(n)=n \tag{1}$$

- logsig

$$\varphi(n)=\frac{1}{1+e^{-n}} \tag{2}$$

- tansig

$$\varphi(n)=\frac{e^{n}-e^{-n}}{e^{n}+e^{-n}} \tag{3}$$

The architecture of three-layer feed-forward neural network used herein presented in Fig. 1 takes one output layer and two hidden layers. In this study the output of the third layer, a^3, was the network output, and this output was labeled as y. In this figure, the input vector P which is an R length input vector is shown by the solid upright block at the left. This network has S^1 neurons in the first layer (hidden layer #1), S^2 neurons in the second layer (hidden layer #2) and S^3 neurons in the third layer (output layer), as above mentioned it is assumed $S^3=1$.

Parts of each layer contains the weight matrix w^i, the multiplication operation, the bias vector b^i, the summer and the transfer function φ^i, where superscript i assigns *i*th layer. The sizes of the matrices are presented just below their matrix variable names.

Bias is an extra input, which takes a value of 1 and is dealt with like other weights [13]. The reason for adding the bias term is that it will allow the network to produce arbitrary outputs different from the defaults, which may be critical for successful learning and weights are adjustable coefficients that decide the intensity of the input signal [75].

Note that w^i and b^i are both changeable parameters of the neuron. The main idea of neural networks is that such parameters can

be modified so that the network function approximates a given function as closely as possible. Thus, during training the weights and biases of the network are systematically adjusted to minimize the network performance function (error function). The performance function of ANN model in this study is sum square error (*SSE*) — the sum of squared error between the ANN outputs and the target outputs (supervised training). There are many different types of training algorithms. Back-propagation, which is a supervised training algorithm, is one of the most commonly used method for training feed-forward neural networks [4,14]. Mathematical aspects of several different training algorithms are described in the literature [7,22,35,58].

RESULTS AND DISCUSSION

1. Statistical Criteria

The reliability and accuracy of the ANN model is based on diverse statistical quantities: Mean square error (MSE); Mean absolute error (MAE); Mean relative squared error (MRSE); Mean relative absolute error (MRAE); Coefficient of Determination (R^2); Correlation Coefficient (R); Accuracy Factor (A_f) and Bias Factor (B_f) given by the following formulas:

$$MSE = \frac{1}{N}\sum_{i=1}^{N}(y_i^{exp} - y_i^{cal})^2 \tag{4}$$

$$MAE = \frac{1}{N}\sum_{i=1}^{N}\left|y_i^{exp} - y_i^{cal}\right| \tag{5}$$

$$MRSE = \frac{1}{N}\sum_{i=1}^{N}\left(\frac{y_i^{exp} - y_i^{cal}}{y_i^{exp}}\right)^2 \tag{6}$$

$$MRAE = \frac{1}{N}\sum_{i=1}^{N}\left|\frac{y_i^{exp} - y_i^{cal}}{y_i^{exp}}\right| \tag{7}$$

$$RAE = \sum_{i=1}^{N}\left|\frac{y_i^{exp} - y_i^{cal}}{y_i^{exp}}\right| \tag{8}$$

$$R^2 = 1 - \frac{\Sigma_{i=1}^{N}(y_i^{exp} - y_i^{cal})^2}{\Sigma_{i=1}^{N}(y_i^{exp} - \overline{y^{exp}})^2} \tag{9}$$

$$R = \left(\left[\sum_{i=1}^{N}(y_i^{exp} - \overline{y^{exp}}) \times (y_i^{cal} - y^{cal})\right] \Big/ \left[\sqrt{\sum_{i=1}^{N}(y_i^{exp} - \overline{y^{exp}})^2} \times \sqrt{\sum_{i=1}^{N}(y_i^{cal} - y^{cal})^2}\right]\right) \tag{10}$$

$$A_f = 10^{\left(\frac{\Sigma_{i=1}^{N}\left|\log\frac{y_i^{cal}}{y_i^{exp}}\right|}{N}\right)} \tag{11}$$

$$B_f = 10^{\left(\frac{\Sigma_{i=1}^{N}\log\frac{y_i^{cal}}{y_i^{exp}}}{N}\right)} \tag{12}$$

where N is the number of data points (input and output pairs), y^{exp} is the value of experimental data sets at the sampling point i, y_i^{cal} is the ith value of the ANN predicted datasets and $\overline{y^{exp}}$ and $\overline{y^{cal}}$ are the average of the experimental and predicted data using the ANN model, respectively, which are defined as:

$$\overline{y^{exp}} = \frac{1}{N}\sum_{i=1}^{N} y_i^{exp} \tag{13}$$

$$\overline{y^{cal}} = \frac{1}{N}\sum_{i=1}^{N} y_i^{cal} \tag{14}$$

Furthermore, the criteria suggested by researchers [31,69] were used to ensure more validity of the ANN model. These statistics are given as follows:

$$k = \frac{\Sigma y_i^{exp} y_i^{cal}}{\Sigma (y_i^{cal})^2} \tag{15}$$

$$k' = \frac{\Sigma y_i^{exp} y_i^{cal}}{\Sigma (y_i^{exp})^2} \tag{16}$$

$$0.85 \le k \le 1.15 \tag{17}$$

$$0.85 \le k' \le 1.15 \tag{18}$$

$$R_o^2 = 1 - \frac{\Sigma (y_i^{cal} - k y_i^{cal})^2}{\Sigma (y_i^{cal} - \overline{y^{cal}})^2} \tag{19}$$

$$R'^2_o = 1 - \frac{\Sigma (y_i^{exp} - k' y_i^{exp})^2}{\Sigma (y_i^{exp} - \overline{y^{exp}})^2} \tag{20}$$

$$m = \frac{R^2 - R_o^2}{R^2} \le 0.1 \tag{21}$$

$$n = \frac{R^2 - R'^2_o}{R^2} \le 0.1 \tag{22}$$

$$R_m^2 = R^2 \times \left(1 - \sqrt{\left|R^2 - R_o^2\right|}\right) \ge 0.5 \tag{23}$$

These parameters are defined to substantiate the validity of the ANN model and indicate whether this model can be applied to estimate desired surface tension of studied binary mixtures containing ILs.

Most of these statistics are discussed in greater detail in the literature [95]; in the context of forecasting; different statistics are also discussed in previous published papers [56,57]. However, A_f and B_f are less introduced in the texts, so a brief description of these statistics is given in the following.

The A_f and B_f were proposed by Ross [73] as criteria for assessing of model performance. The overall agreement between estimated and actual values is indicated by the B_f value. It will specify whether the estimations lie averagely above or below the line of equivalence, and by how much. Equal weighting is specified to overestimation, where the estimated value is greater than the actual one, and under-estimation. The B_f is defined with the Eq. (12) [8].

A B_f of 1 means complete agreement. A value larger than 1 would show that, on average, the estimations were larger than the actual values and would stand for a fail-dangerous model; for instance a

Table 3. Effects of number of hidden neurons in hidden layer(s) on MSE and R

	Network topology	MSE				R			
		All	Training	Validation	Testing	All	Training	Validation	Testing
1	6-2-1	1.4401E-05	1.4093E-05	1.4871E-05	1.5375E-05	0.9274	0.9303	0.9215	0.9169
2	6-3-1	1.1431E-05	1.0746E-05	1.2073E-05	1.3996E-05	0.9428	0.9486	0.9372	0.9145
3	6-4-1	9.5883E-06	7.7913E-06	1.6421E-05	1.1162E-05	0.9523	0.9615	0.9116	0.9491
4	6-5-1	5.3160E-06	5.5469E-06	3.9181E-06	5.6339E-06	0.9738	0.9752	0.9738	0.9653
5	6-6-1	4.6725E-06	4.7307E-06	4.8465E-06	4.2265E-06	0.9770	0.9780	0.9755	0.9750
6	6-7-1	3.0219E-06	2.3196E-06	6.6009E-06	2.7282E-06	0.9852	0.9891	0.9661	0.9849
7	6-8-1	2.1344E-06	2.1345E-06	2.2948E-06	1.9734E-06	0.9896	0.9902	0.9872	0.9890
8	6-9-1	1.8278E-06	1.7513E-06	1.7878E-06	2.2257E-06	0.9911	0.9918	0.9897	0.9892
9	6-10-1	1.7327E-06	1.7408E-06	1.9844E-06	1.4431E-06	0.9915	0.9917	0.9910	0.9907
10	6-11-1	1.4125E-06	1.2951E-06	1.6112E-06	1.7631E-06	0.9931	0.9934	0.9926	0.9923
11	6-12-1	1.2205E-06	1.1311E-06	1.4053E-06	1.4541E-06	0.9941	0.9947	0.9920	0.9932
12	6-13-1	1.2633E-06	1.1849E-06	1.7061E-06	1.1874E-06	0.9938	0.9943	0.9930	0.9927
13	6-14-1	1.1213E-06	1.0385E-06	1.3613E-06	1.2686E-06	0.9945	0.9950	0.9928	0.9941
14	6-15-1	9.4381E-07	8.2422E-07	1.5736E-06	8.7351E-07	0.9954	0.9960	0.9923	0.9957
15	6-16-1	9.8200E-07	8.3731E-07	6.7071E-07	1.9702E-06	0.9952	0.9961	0.9957	0.9907
16	6-17-1	8.3066E-07	7.5134E-07	1.0103E-06	1.0221E-06	0.9960	0.9964	0.9940	0.9954
17	6-18-1	7.9155E-07	5.4823E-07	1.6101E-06	1.1114E-06	0.9961	0.9974	0.9932	0.9935
18	6-19-1	8.2842E-07	7.1467E-07	1.0061E-06	1.1830E-06	0.9960	0.9966	0.9945	0.9943
19	6-20-1	7.8904E-07	6.8972E-07	9.9947E-07	1.0433E-06	0.9962	0.9967	0.9957	0.9947
20	6-2-2-1	1.0721E-05	9.4547E-06	1.8269E-05	9.0961E-06	0.9465	0.9531	0.9217	0.9457
21	6-3-3-1	6.6121E-06	5.9846E-06	7.7295E-06	8.4306E-06	0.9673	0.9692	0.9636	0.9630
22	6-4-4-1	2.5976E-06	2.3775E-06	3.0075E-06	3.2172E-06	0.9873	0.9880	0.9849	0.9865
23	6-5-5-1	1.5708E-06	1.4778E-06	1.6448E-06	1.9321E-06	0.9923	0.9928	0.9926	0.9913
24	6-6-6-1	7.8659E-07	6.8052E-07	1.3017E-06	7.6776E-07	0.9962	0.9965	0.9948	0.9962
25	6-7-7-1	7.2295E-07	6.7236E-07	8.4137E-07	8.4122E-07	0.9965	0.9967	0.9961	0.9960
26	6-8-8-1	3.0665E-07	2.7575E-07	4.5942E-07	2.9845E-07	0.9985	0.9987	0.9976	0.9984
27	6-9-9-1	1.5138E-07	1.2080E-07	2.0690E-07	2.3892E-07	0.9993	0.9994	0.9991	0.9987
28	6-10-10-1	1.3436E-07	1.2804E-07	1.3772E-07	1.6060E-07	0.9993	0.9994	0.9994	0.9992
29	6-11-11-1	1.3168E-07	8.8461E-08	1.3877E-07	3.2678E-07	0.9994	0.9996	0.9992	0.9988
30	6-12-12-1	8.7914E-08	7.3271E-08	7.3665E-08	1.7067E-07	0.9996	0.9996	0.9996	0.9993
31	6-13-13-1	3.5358E-07	2.6944E-07	7.3166E-07	3.6915E-07	0.9983	0.9987	0.9963	0.9984
32	6-14-14-1	3.6125E-07	2.8248E-07	6.4388E-07	4.4714E-07	0.9982	0.9986	0.9974	0.9979
33	6-15-15-1	3.7344E-07	2.9223E-07	7.5284E-07	3.7397E-07	0.9982	0.9985	0.9970	0.9984

Table 4. Effect of training algorithm on network performance

	Training algorithm	MSE				R			
		All	Training	Validation	Testing	All	Training	Validation	Testing
1	Trainbfg	1.2476E-05	1.0608E-05	1.1083E-05	2.2608E-05	0.9375	0.9469	0.9439	0.8858
2	Trainbr	8.7914E-08	7.3271E-08	7.3665E-08	1.7067E-07	0.9996	0.9996	0.9996	0.9993
3	Traincgb	8.3442E-06	7.6229E-06	7.7799E-06	1.2283E-05	0.9586	0.9635	0.9588	0.9318
4	Traincgf	1.2838E-05	1.3182E-05	1.2427E-05	1.1639E-05	0.9356	0.9377	0.9317	0.9257
5	Traincgp	8.8324E-06	7.3462E-06	9.6662E-06	1.4952E-05	0.9562	0.9625	0.9535	0.9335
6	Traingda	3.0531E-05	2.9031E-05	3.7833E-05	3.0249E-05	0.8457	0.8606	0.7951	0.8187
7	Traingdx	2.6303E-05	2.6210E-05	2.9483E-05	2.3557E-05	0.8683	0.8732	0.8520	0.8565
8	Trainlm	6.6522E-07	2.9835E-07	2.3194E-06	7.2743E-07	0.9968	0.9985	0.9900	0.9963
9	Trainoss	1.9678E-05	1.9742E-05	1.7913E-05	2.1142E-05	0.9009	0.9069	0.8890	0.8828
10	Trainrp	6.5366E-06	6.0244E-06	9.8420E-06	5.6275E-06	0.9677	0.9703	0.9558	0.9702
11	Trainscg	7.6698E-06	7.7182E-06	8.0997E-06	7.0135E-06	0.9620	0.9626	0.9612	0.9609

B_f of 1.3 would show that the estimations were 30% larger than actual values [8]. A value less than 1 would show a fail-safe model where, on average, the estimations were shorter than actual values. The over (+) and under (–) estimations can negate each other during calculation of the B_f. They do not then show the absolute errors in the model. This goal can be attained by the use of the A_f (accuracy factor). This is based on a similar equation to (19) but ignores whether the difference between the estimated and actual value is positive or negative.

The A_f value will always be equal to (if there is perfect agreement) or greater than one as all variances are positive. The A_f value of 1.4 indicates that, on average, the estimated value is 40% different (either larger or smaller) from the actual value.

In short, the SGB predictions are ideal if MSE, MAE, MRSE, MRAE, R^2, R, A_f and B_f are found to be close to 0, 0, 0, 0, 1, 1, 1 and 1, respectively.

2. Creating an ANN Model

The aim of the study was to build a model, capable of predicting the surface tension of binary mixtures containing ILs as dependent variable. It is supplied by the T, x_{IL}, Mw_{IL} and ρ_{IL} along with $Tb_{non\text{-}IL}$ and $Mw_{non\text{-}IL}$ data as independent variables (input arguments). ANN was used as the prediction technique to carry out the task.

Table 5. Optimal values of weights and biases obtained during ANN training

Input weight matrix destination: hidden layer #1; Source: inputs

$$w^1 = \begin{bmatrix} 0.1175 & 0.4646 & 1.2032 & -1.5219 & -3.2049 & 1.1517 \\ 0.3957 & 0.8603 & 1.3409 & -2.2488 & -1.7823 & 0.5923 \\ 0.4073 & -9.8283 & 3.0883 & 2.3222 & -2.0155 & 0.1361 \\ -0.3802 & 1.6325 & -0.6590 & -0.0858 & 0.8652 & 1.4491 \\ -0.2004 & -2.7077 & -1.8364 & -1.7052 & -1.2306 & -0.0403 \\ -0.0995 & 0.4371 & 0.0824 & 2.3188 & 0.6802 & 0.2481 \\ 0.0435 & 0.1233 & 1.5630 & 0.8628 & -2.4379 & 0.2780 \\ -0.8408 & -0.5287 & -2.7406 & -2.5344 & 0.8479 & -0.2260 \\ 0.3373 & 2.2723 & 2.1543 & -2.2708 & 0.7429 & -2.9994 \\ 0.0893 & -0.2943 & -0.8918 & 0.7854 & 0.0499 & -0.6965 \\ 0.1157 & -0.7054 & 0.4832 & 0.0708 & 1.5824 & -0.9099 \\ 0.5157 & 10.8179 & 4.2810 & 2.9734 & -3.6468 & -2.4995 \end{bmatrix}$$

Layer weight matrix destination: hidden layer #2; Source: hidden layer #1

$$w^2 = \begin{bmatrix} 0.0563 & -0.3205 & 0.2805 & -0.1819 & -0.1389 & 1.6434 & -0.1792 & 0.0627 & -0.0347 & 1.1277 & -0.2592 & -1.3123 \\ 0.0115 & 1.2863 & -0.3544 & 0.3923 & -0.1260 & 1.2873 & 0.0669 & 1.8359 & -0.1140 & 0.0877 & -0.1272 & -0.2181 \\ 0.0551 & 1.0692 & -0.2998 & 1.0509 & -0.2809 & 1.5626 & 0.0738 & 0.6774 & -0.1789 & 0.2285 & -0.2578 & -0.2103 \\ -0.1007 & -0.4720 & 10.3768 & 0.1789 & -0.0206 & -0.8154 & 1.4072 & 0.7920 & 4.0085 & 0.6788 & -2.3345 & -10.8589 \\ -0.8379 & 0.3847 & -8.6672 & -4.4612 & 2.0421 & -0.0674 & 0.8113 & -1.8946 & -2.9053 & 0.5852 & 3.0063 & 8.2085 \\ -0.2034 & 0.0437 & 1.1131 & -0.3224 & -0.9284 & 0.6781 & 0.1512 & -0.4754 & 0.3608 & -0.7860 & -0.6866 & 0.1339 \\ 0.8447 & -0.1144 & 0.0579 & -0.4727 & 0.5599 & 1.1139 & -0.1848 & 2.1465 & 0.5442 & -0.5484 & 1.0438 & 0.4132 \\ -0.9713 & 0.8580 & -0.8116 & 0.1676 & 0.7223 & 0.6772 & 0.8171 & 0.1685 & -0.1266 & -0.1849 & -1.0291 & -0.3906 \\ -1.1275 & -1.0061 & -1.2611 & 0.2740 & -0.4977 & 1.3262 & 1.6710 & 1.1292 & -0.1942 & 1.4318 & 1.3098 & 0.4365 \\ 0.1013 & 0.5021 & -0.1369 & -0.1989 & 0.5345 & 0.5707 & 0.0662 & -0.9548 & 0.2810 & 0.2502 & -0.3053 & -0.2142 \\ -0.1969 & -0.7450 & 0.5015 & 0.7148 & 1.2064 & -1.3904 & 1.1691 & 0.6759 & 0.2780 & -1.1109 & 0.7267 & 1.4307 \\ -0.6868 & -1.4973 & 1.0003 & 0.0656 & -0.0223 & 1.2401 & 0.8945 & 0.3966 & 0.0029 & 1.2263 & -0.1860 & -1.2068 \end{bmatrix}$$

Layer weight vector destination: Output Layer; Source: hidden layer #2

$$w^3 = [\,1.4180 \quad -3.2917 \quad 2.6890 \quad -2.8796 \quad -8.2024 \quad 0.8980 \quad 2.8720 \quad 0.8641 \quad -0.6091 \quad -0.9566 \quad 0.5293 \quad -0.9184\,]$$

Bias vector destination: Hidden Layer #1

$$b^1 = [\,-0.6228 \quad -2.2896 \quad -8.2126 \quad -0.6068 \quad 0.4720 \quad 2.4934 \quad -0.0011 \quad -1.7273 \quad -0.3188 \quad -0.1550 \quad 0.2403 \quad 10.6928\,]^T$$

Bias vector destination: Hidden Layer #2

$$b^2 = [\,0.0463 \quad 0.0666 \quad 2.1364 \quad -0.7053 \quad -3.7678 \quad 0.2872 \quad -0.3797 \quad -0.3838 \quad -0.6307 \quad -0.6374 \quad -0.7568 \quad -0.0101\,]^T$$

Bias scalar destination: Output Layer

$$b^3 = [2.4181]$$

70% (524 data points out of a total of 748 data points) and 15% of the data were, respectively, used to train and validate the network and the rest is put aside for testing the trained network.

Finding a suitable ANN architecture is of central importance due to its major effects on the produced results. However, the optimal architecture (the number of hidden layers and neurons within each layer), is problem specific and needs the trial and error approach. Small network cannot be trained with desirable and high accuracy. On the other hand, an overly complex network becomes noise dependent. Table 3 presents the performance of different configurations of ANN models with different number of neurons in the hidden layers for one and two hidden layer structures. Owing to the impact of initial weights on model performance, 20 runs were performed for each network structure. Then, the best trained network was chosen as an optimum one. According to the statistical analysis results, a network with two hidden layers is the optimal network structure containing twelve neurons in both hidden layers.

There are many learning algorithms which update network weight and bias. Table 4 shows the effect of use of various training algorithms on the network prediction performance. The studied learning algorithms herein are: BFGS quasi-Newton backpropagation (trainbfg), trainbr, Powell-Beale conjugate gradient backpropagation (traincgb), Fletcher-Powell conjugate gradient backpropagation (traincgf), Polak-Ribiére conjugate gradient backpropagation (traincgp), Gradient descent with adaptive learning rule backpropagation (traingda), Gradient descent with momentum and adaptive learning rule backpropagation (traingdx), Levenberg-Marquardt backpropagation (trainlm), One step secant backpropagation (trainoss),

Table 6. Details of the obtained error analysis for each investigated binary system

No.	Binary system	MRAE	R	B_f	A_f	RAE	
						Min	Max
1	1-Octene/[HMIM] [TF2N]	0.0078598	0.9970812	1.0000778	1.0078915	0.0002617	0.0231721
2	Dimethyl sulfoxide/[BMIM] [TF2N]	0.0020092	0.9993311	0.9999487	1.0020124	0.0000638	0.0121864
3	Dimethyl sulfoxide/[EMIM] [TF2N]	0.0022999	0.9987286	0.9999753	1.0023024	0.0001170	0.0064810
4	Acetonitrile/[BMIM] [TF2N]	0.0019477	0.9988967	0.9998361	1.0019498	0.0001082	0.0059617
5	Tetrahydrofuran/[BMIM] [TF2N]	0.0015893	0.9994814	0.9999434	1.0015903	0.0001122	0.0079979
6	Methanol/[BMIM][L-lactate]	0.0033384	0.9998234	0.9999396	1.0033443	0.0003308	0.0082174
7	Water/[BMIM][L-lactate]	0.0041841	0.9992998	1.0000011	1.0041936	0.0000860	0.0176242
8	1-Butanol/[BMIM][L-lactate]	0.0038115	0.9996236	1.0000205	1.0038173	0.0000254	0.0165081
9	Ethanol/[BMIM][L-lactate]	0.0036234	0.9997985	1.0000557	1.0036304	0.0002938	0.0097373
10	Water/[BMIM] [BF_4]	0.0096630	0.9861769	1.0002559	1.0096862	0.0000669	0.0637528
11	Water/[EMIM] [BF_4]	0.0037216	0.9985736	0.9999654	1.0037257	0.0004452	0.0120364
12	Ethanol/[BMIM] [BF_4]	0.0076920	0.9992201	1.0010296	1.0077193	0.0016520	0.0170804
13	Ethanol/[HMIM] [BF_4]	0.0063175	0.9990704	0.9991971	1.0063468	0.0015640	0.0144016
14	Ethanol/[OMIM] [BF_4]	0.0042477	0.9989667	1.0018500	1.0042465	0.0002983	0.0123116
15	Water/[HMIM] [BF_4]	0.0028144	0.8105856	0.9988301	1.0028232	0.0005576	0.0089302
16	Ethanol/[EMIM] [BF_4]	0.0044801	0.9995208	1.0003688	1.0044817	0.0000165	0.0121983
17	Water/[EMIM][BS]	0.0100995	0.9277086	1.0004031	1.0101581	0.0000575	0.0279926
18	Water/[EMIM][OS]	0.0043715	0.9994442	0.9999150	1.0043803	0.0005507	0.0137550
19	Water/[EMIM][HS]	0.0043426	0.9996848	0.9999823	1.0043521	0.0002940	0.0090474
20	Ethanol/[EMIM][OS]	0.0023309	0.9994483	1.0003342	1.0023336	0.0001549	0.0067161
21	Water/[EMIM][ES]	0.0027608	0.9997536	0.9999257	1.0027655	0.0000243	0.0055502
22	Ethanol/[EMIM][HS]	0.0042473	0.9994116	0.9983632	1.0042619	0.0010732	0.0091980
23	Ethanol/[EMIM][ES]	0.0031598	0.9999079	0.9991681	1.0031693	0.0004546	0.0078215
24	Ethanol/[EMIM][BS]	0.0040642	0.9994574	1.0006696	1.0040689	0.0003351	0.0110019
25	1-Butanol/[BMIM] [TF2N]	0.0051579	0.9988538	0.9991892	1.0051743	0.0012166	0.0124764
26	1-Propanol/[BMIM] [TF2N]	0.0047864	0.9990546	1.0011243	1.0047925	0.0006275	0.0096051
27	Methanol/[EMIM][MS]	0.0043936	0.9998081	0.9999487	1.0043971	0.0004476	0.0169095
28	Ethanol/[EMIM][MS]	0.0040037	0.9998347	1.0000545	1.0040099	0.0000006	0.0132884
29	1-Butanol/[EMIM][MS]	0.0071602	0.9993916	1.0000977	1.0071717	0.0000975	0.0251925
30	Water/[EMIM][L-lactate]	0.0068524	0.9955055	1.0000341	1.0068720	0.0016862	0.0216618
31	Water/[BMIM][Glu]	0.0047556	0.9983140	0.9999608	1.0047698	0.0000257	0.0125535
	All dataset	MRAE	R	B_f	A_f	RAE	
						Min	Max
		0.0042650	0.9995726	1.0000057	1.0042731	0.0000006	0.0637528

Resilient backpropagation (trainrp), Scaled conjugate gradient backpropagation (trainscg). From the results it can be confirmed that the optimum training function is 'trainbr' and the optimum values of weights and biases of ANN architecture shown in Fig. 1, are summarized in Table 5. Consequently, the ANN model for the prediction of binary surface tension can be described as a composite mapping:

$$Y=\varphi^3(w^3(\varphi^2(w^2(\varphi^1(w^1x+b^1))+b^2))+b^3) \quad (24)$$

As described in previous section φ^i is the vector of transfer function corresponding to layer i (i=1-3) and the other terms i.e. w^i, b^i and x stand for the weights, biases and inputs, respectively.

3. Results of the Used ANN Model

The criteria including R, B_f, A_f and MRAE along with maximum and minimum values of RAE for different binary systems were calculated and presented in Table 6. The obtained results which were given in Table 6 revealed that the ANN model is capable of estimating the binary surface tension of the ILs mixtures regarding to all of the concerned systems with the R, B_f, A_f and MRAE of 0.9995726, 1.0000057, 1.0042731 and 0.0042650 respectively.

Also the MSE, MAE, MRSE, MRAE, R^2, k, k′, m and n as well as R_m^2 values for all data sets including training, validation and testing are shown in Table 7. As can be seen, the high ability and validity of the ANN model is clearly shown.

The regression plots, shown in Fig. 2, show the ANN predictions with respect to experimental values for all three data sets, i.e., training, validation, and test sets. For an ideal fit, the points should lie along a 45° line, where the ANN estimations are equal to the actual values. As shown, the results are very good for three data sets as R values in each case are 0.99929 or above.

Table 7. Calculated values of different statistics for the training, validation and test data set

	Training data	Validation data	Testing data
MSE	7.32707E-08	7.36649E-08	1.70672E-07
MAE	1.60619E-04	1.84412E-04	1.52674E-04
MRSE	4.02002E-05	3.80531E-05	5.66226E-05
MRAE	4.30232E-03	4.51578E-03	3.82851E-03
R	9.99641E-01	9.99625E-01	9.99293E-01
R^2	9.99283E-01	9.99250E-01	9.98587E-01
B_f	9.99749E-01	1.00013E+00	1.00108E+00
A_f	1.00431E+00	1.00453E+00	1.00385E+00
k	1.00043E+00	1.00020E+00	9.97914E-01
k′	9.99523E-01	9.99751E-01	1.00197E+00
m	−7.15405E-04	−7.49547E-04	−1.36117E-03
n	−7.14767E-04	−7.49211E-04	−1.36623E-03
R_m^2	9.72564E-01	9.71903E-01	9.61771E-01

3D illustration of surface tension of binary mixtures as a function of IL concentration and temperature for different binary systems is in Figs. 3-5. According to the figures, the goodness of ANN approach to predict solubility of surface tension of binary mixtures is acceptable for the whole range of temperature and IL concentration.

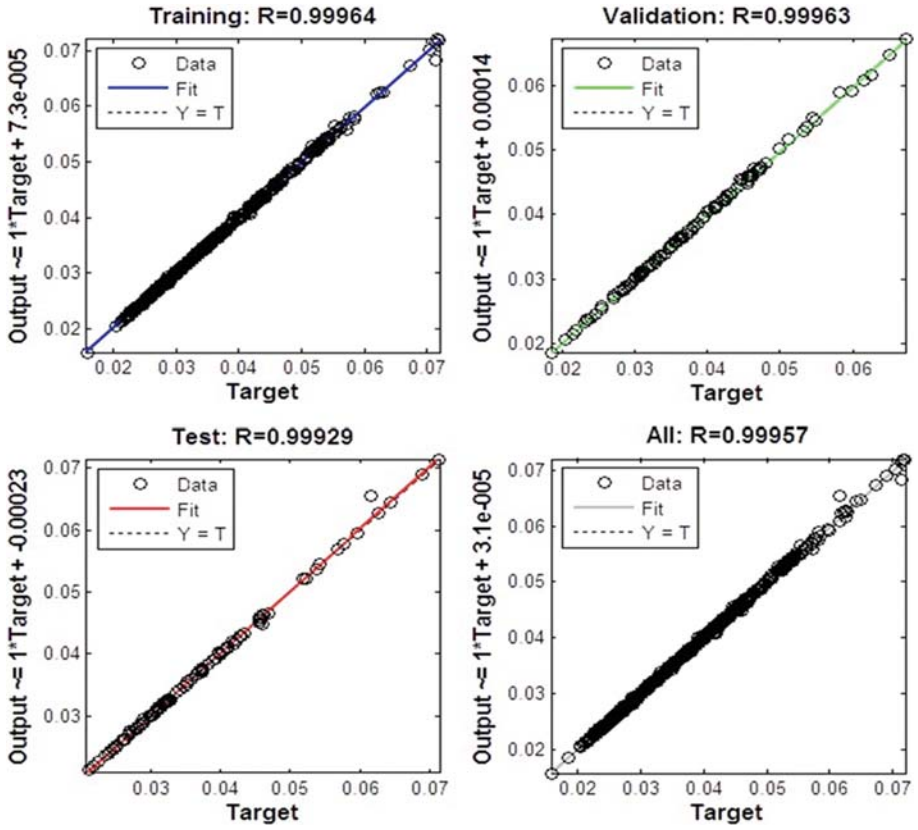

Fig. 2. Regression plots of ANN for prediction of surface tension of binary systems containing ILs.

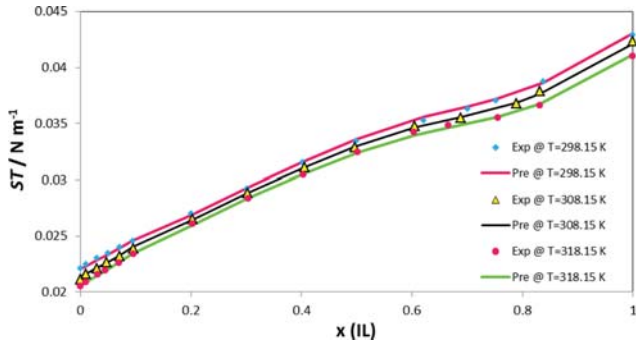

Fig. 3. 3D diagram of surface tension of binary mixture ethanol & [BMIM][L-lactate] as a function of temperature and concentration of IL component.

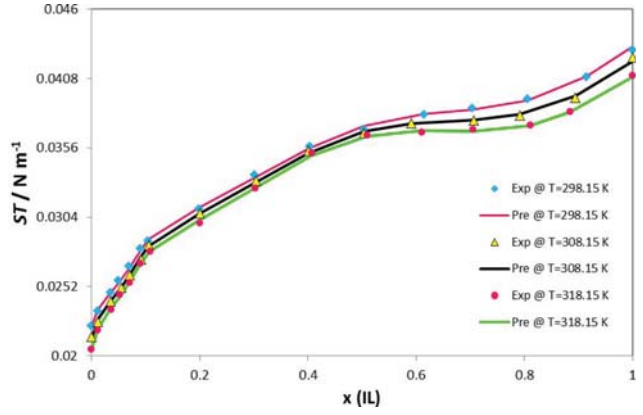

Fig. 4. 3D diagram of surface tension of binary mixture methanol & [BMIM][L-lactate] as a function of temperature and concentration of IL component.

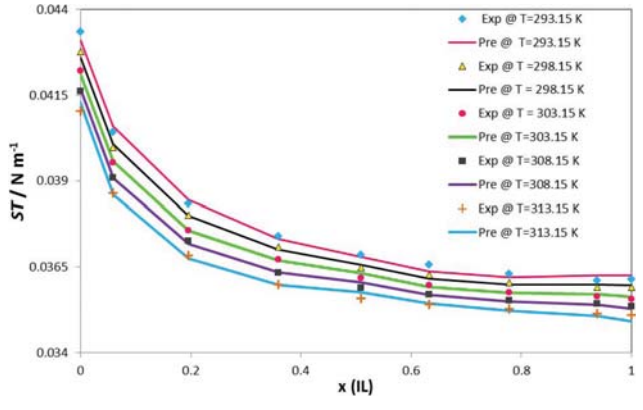

Fig. 5. 3D diagram of surface tension of binary mixture dimethyl sulfoxide & [EMIM][TF2N] as a function of temperature and concentration of IL component.

Furthermore, Fig. 6 shows the RAE% of all data points in the form of the percentage samples in each range of RAE%. As shown, 92.25% ANN predictions were in the error range of 0-1% and 0.13% of ANN model prediction had errors exceeding 6% and the maximum RAE% was 6.37%. Taking all above-mentioned considerations into account, it can be concluded that the ANN model

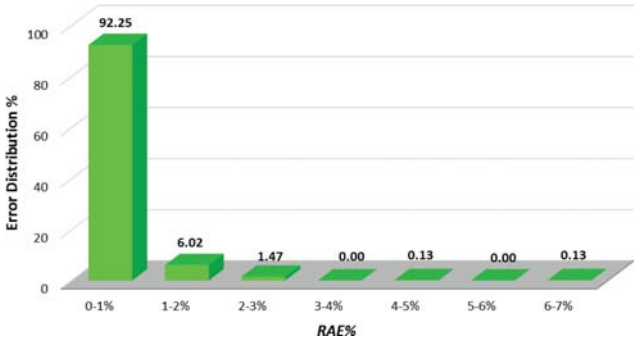

Fig. 6. Distribution of the *RAE*% of the ANN outputs from the corresponding experimental values of binary surface tension.

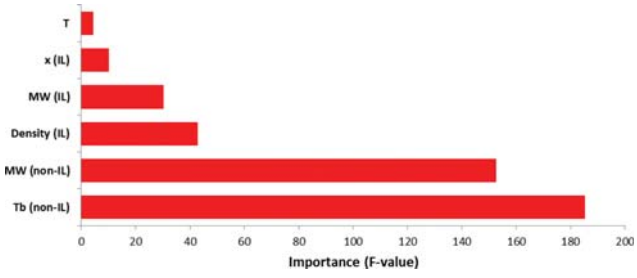

Fig. 7. Relative importance of input parameters on dependent variable (surface tension of binary mixtures).

can be used as a very competent and highly precise scheme to predict the surface tension of binary systems containing ILs.

To determine relative importance of the input variables on the desired target of this study that is surface tension of IL binary mixtures, a statistical method has been implemented. The obtained results from the statistical analysis are exhibited in Fig. 7. As shown, the normal boiling point of non-IL component has the highest effect on the surface tension of investigated binary systems based on F value.

4. Comparison of the Used Model vs. the Others

The capability and feasibility of the used ANN model for predicting the surface tension of different binary systems containing ILs was compared to other computational intelligence schemes including support vector machine (SVM), least squared support vector machine optimized by genetic algorithm (GA-LSSVM) and least squared support vector machine optimized by coupled simulated annealing (CSA-LSSVM) [34] from MRAE point of view. Error analysis reported in Table 8 shows that the proposed ANN prediction model which was trained by trainbr (MRAE% of 0.44) appears more competent to correlate the binary surface tension compared with the three models of ANN with one hidden layer trained by trainlm algorithm (MRAE % of 1.06) [46], SVM (MRAE % of 3.71) [34], CSA-LSSVM (MRAE% of 1.07) [34] and GA-LSSVM (MRAE % of 1.87) [34] based on the same data for 21 distinct binary systems. Note that the ANN which used *trainlm* as learning algorithm [46] considered temperature, mole fraction together with the melting point and molecular weight of the IL and non-IL components as model input variables to differentiate between the various compounds involved in binary systems, while the density of IL

Table 8. Comparison of the used ANN algorithm with other methods in terms of MRAE%

No.	Binary system	MRAE%				
		ANN [46] trained with trainlm	SVM [34]	GA-LSSVM [34]	CSA-LSSVM [34]	ANN trained with trainbr
1	1-Octene/[HMIM] [TF2N]	2.07	3.12	0.98	1.09	0.79
2	Dimethyl sulfoxide/[BMIM] [TF2N]	0.34	1.77	1.53	0.62	0.20
3	Dimethyl sulfoxide/[EMIM] [TF2N]	0.34	2.81	0.92	0.20	0.23
4	Acetonitrile/[BMIM] [TF2N]	0.41	3.32	0.72	0.18	0.19
5	Tetrahydrofuran/ [BMIM] [TF2N]	1.30	2.61	0.23	0.24	0.16
6	Water/[BMIM] [BF_4]	2.62	5.56	5.88	4.05	0.97
7	Water/[EMIM] [BF_4]	0.87	3.48	3.90	1.70	0.37
8	Ethanol/[BMIM] [BF_4]	0.66	3.80	1.71	0.93	0.77
9	Ethanol/[HMIM] [BF_4]	1.28	2.06	0.42	0.58	0.63
10	Ethanol/[OMIM] [BF_4]	0.81	1.85	0.45	0.15	0.42
11	Water/[HMIM] [BF_4]	0.25	2.28	0.13	0.01	0.28
12	Ethanol/[EMIM] [BF_4]	0.58	12.22	2.60	0.25	0.45
13	Water/[EMIM] [OS]	2.39	5.73	5.59	4.66	0.44
14	Ethanol/[EMIM] [OS]	0.23	2.00	0.74	0.14	0.23
15	Water/[EMIM] [ES]	1.12	5.94	3.18	1.51	0.28
16	Ethanol/[EMIM] [ES]	0.49	1.89	0.20	0.41	0.32
17	1-Butanol/[BMIM] [TF2N]	2.14	2.59	1.33	0.39	0.52
18	1-Propanol/[BMIM] [TF2N]	1.63	2.91	0.81	1.46	0.48
19	Methanol/[EMIM] [MS]	0.96	3.07	0.80	0.34	0.44
20	Ethanol/[EMIM] [MS]	0.55	3.06	1.51	0.46	0.40
21	1-Butanol/[EMIM] [MS]	1.32	5.88	5.73	3.04	0.72
	Average	1.06	3.71	1.87	1.07	0.44

and boiling point temperature of non-IL instead of melting point of IL and non-IL components were selected in this study the same as SVM, GA-LSSVM and CSA-LSSVM models [34]. Although Lashkarbolooki [46] used a simpler network (with one hidden layer instead of two) than the current model, the ANN model trained by trainbr in this study yielded more accurate outputs.

Moreover, three prediction models proposed by Atashrouz et al. [6], named GA-SVM, GA-LSSVM and group method of data handling type polynomial neural network (GMDH-PNN), which considered temperature, mole fraction of IL, together with the surface tension of pure components as model input variables, were selected as comparative models in order to show the advances and signifi-

Table 9. Comparison of the GA-SVM, GA-LSSVM, GMDH-PNN [6] and ANN models for prediction of surface tension of 13 binary mixtures

No.	Binary system	MRAE%			
		GA-LSSVM	GA-SVM	GMDH-PNN	ANN
1	Dimethyl sulfoxide/[BMIM] [TF2N]	0.58	0.92	2.45	0.20
2	Dimethyl sulfoxide/[EMIM] [TF2N]	0.37	0.68	1.74	0.23
3	Acetonitrile/[BMIM] [TF2N]	0.56	0.91	2.60	0.19
4	Tetrahydrofuran/[BMIM] [TF2N]	0.82	0.83	1.30	0.16
5	Ethanol/[BMIM] [BF_4]	2.57	0.88	7.87	0.77
6	Ethanol/[HMIM] [BF_4]	1.12	0.55	3.10	0.63
7	Ethanol/[OMIM] [BF_4]	3.54	3.48	1.35	0.42
8	Water/[HMIM] [BF_4]	3.67	5.94	1.48	0.28
9	Water/[EMIM] [BS]	1.02	0.96	2.26	1.01
10	Ethanol/[EMIM] [OS]	1.36	1.09	3.30	0.23
11	Ethanol/[EMIM] [HS]	1.61	1.43	2.76	0.42
12	1-Butanol/[BMIM] [TF2N]	3.27	2.45	8.22	0.52
13	1-Propanol/[BMIM] [TF2N]	0.94	1.56	3.40	0.48
	Average	1.65	1.67	3.22	0.43

cance of the ANN model in the current research based on the same data for 13 distinct binary systems. Table 9 indicates the proposed ANN model in this study has lower MRAE% value against others. Atashrouz et al. [6] developed two different models for organic based mixtures and water based mixtures, while in this study just one integrated model based ANN which can be successfully used for both organic based mixtures and water based mixtures, presented.

Apparently, from the figures and statistical analyses, the proposed model exhibits the best performances for such prediction. As shown in Tables 8 and 9, we can note the superiority of the ANN with two hidden layers and *trainbr* as training function to SVM, GA-LSSVM, CSA-LSSVM, ANN trained by trainlm and GMDH-PNN. Statistical criteria presented in Tables 6 and 7 record the proposed model could predict surface tension of binary mixtures containing ILs, with high precision, and the good correlations presented by R and R^2 illustrate that the predicted data are consistent with experimental values.

CONCLUSION

The ANN model with two hidden layers and trained by *trainbr* algorithm has been utilized by for prediction of the surface tension of binary mixtures containing 31 diverse ILs based on the operational temperature (T), the IL component compositions (x_{IL}), molecular weight of IL components (Mw_{IL}) and density of IL components (ρ_{IL}) along with the boiling point ($Tb_{non\text{-}IL}$) and molecular weight ($Mw_{non\text{-}IL}$) of non-IL component. 748 of data points were gathered from diverse literature resources to employ in the ANN model as training, validation and testing data points. The following conclusions can be drawn:

(1) Very reasonable results were obtained with the proposed ANN method. This fact is supported by the acceptable statistical quality confirmed by various parameters, and the low errors of the ANN model results indicate that it can accurately predict the surface tension of binary mixtures including ILs which is of great practical significance.

(2) The binary surface tension predictions trend is also concordant with the experimental.

(3) In addition to the high precision of the obtained results, the most important advantage of the method suggested in this study is that it correlated the values obtained exclusively from experimental data, which is an important feature for the scientific community and engineers in using such model with confidence.

(4) Compared with the traditional computation approaches, such as cubic plus association (CPA) equation of state, PVT corrections caused by the effect of high pressure and temperature are not required in applying ANN model, and give high accuracy. Also, it presents excellent prediction competence and high precision versus other algorithms, such as SVM, GA-SVM, CSA-LSSVM, GA-LSSVM, GMDH-PNN and ANN trained with one hidden layer and *trainlm* as training function.

REFERENCES

1. M.-A. Ahmadi, B. Pouladi, Y. Javvi, S. Alfkhani and R. Soleimani, *J. Supercrit. Fluids*, **97**, 81 (2015).
2. M. A. Ahmadi, R. Haghbakhsh, R. Soleimani and M. B. Bajestani, *J. Supercrit. Fluids*, **92**, 60 (2014).
3. A. Ahosseini, B. Sensenich, L. R. Weatherley and A. M. Scurto, *J. Chem. Eng. Data*, **55**, 1611 (2009).
4. K. A. Al-Shayji, *Modeling, simulation, and optimization of large-scale commercial desalination plants*, Virginia Polytechnic Institute and State University (1998).
5. N. Altinkok and R. Koker, *Mater. Design*, **25**, 595 (2004).
6. S. Atashrouz, H. Mirshekar, A. Hemmati-Sarapardeh, M. K. Moraveji and B. Nasernejad, *Korean J. Chem. Eng.*, **34**(2), 425 (2017).
7. D. R. Baughman and Y. A. Liu, *Neural networks in bioprocessing and chemical engineering*, Academic Press (2014).
8. G. Betts and S. Walker, *Verification and validation of food spoilage models, Understanding and measuring shelf life of food*, CRC Press, Boca Raton, 184 (2004).
9. R. Bini, C. Chiappe, C. Duce, A. Micheli, R. Solaro, A. Starita and M. R. Tiné, *Green Chemistry*, **10**, 306 (2008).
10. R. B. Boozarjomehry, F. Abdolahi and M. A. Moosavian, *Fluid Phase Equilib.*, **231**, 188 (2005).
11. P. J. Carvalho, M. G. Freire, I. M. Marrucho, A. J. Queimada and J. A. Coutinho, *Surface tensions for the 1-alkyl-3-methylimidazolium bis (trifluoromethylsulfonyl) imide ionic liquids* (2008).
12. A. J. Costa, J. M. Esperança, I. M. Marrucho and L. s. P. N. Rebelo, *J. Chem. Eng. Data*, **56**, 3433 (2011).
13. N. Darwish, N. Hilal, H. Al-Zoubi and A. W. Mohammad, *Chem. Eng. Res. Design*, **85**, 417 (2007).
14. H. Demuth, M. Beale and M. Hagan, Neural network toolbox™ 6, *User's guide*, 37 (2008).
15. P. Díaz-Rodríguez, J. C. Cancilla, G. Matute and J. S. Torrecilla, *J. Ind. Eng. Chem.*, **21**, 1350 (2015).
16. B. N. K. L. Ding, *Neural network fundamentals with graphs, algorithms and applications*, Mac Graw-Hill (1996).
17. Q. Dong, C. D. Muzny, A. Kazakov, V. Diky, J. W. Magee, J. A. Widegren, R. D. Chirico, K. N. Marsh and M. Frenkel, *J. Chem. Eng. Data*, **52**, 1151 (2007).
18. A. Eslamimanesh, F. Gharagheizi, A H. Mohammadi and D. Richon, *Chem. Eng. Sci.*, **66**, 3039 (2011).
19. R. Eslamloueyan and M. Khademi, *Int. J. Thermal Sci.*, **48**, 1094 (2009).
20. R. Eslamloueyan and M. H. Khademi, *J. Chem. Eng. Data*, **54**, 922 (2009).
21. M.-R. Fatehi, S. Raeissi and D. Mowla, *J. Supercrit. Fluids*, **95**, 60 (2014).
22. J. A. Freeman and D. M. Skapura, *Algorithms, applications, and programming techniques*, Addison-Wesley Publishing Company, U.S.A. (1991).
23. M. Freemantle, *An introduction to ionic liquids*, Royal Society of Chemistry (2010).
24. F. l. M. Gaciño, T. Regueira, L. Lugo, M. a. J. Comuñas and J. Fernández, *J. Chem. Eng. Data*, **56**, 4984 (2011).
25. G. García-Miaja, J. Troncoso and L. Romaní, *J. Chem. Thermodynamics*, **41**, 161 (2009).
26. M. Geppert-Rybczyńska, J. K. Lehmann, J. Safarov and A. Heintz, *J. Chem. Thermodynamics*, **62**, 104 (2013).
27. F. Gharagheizi, A. Eslamimanesh, A. H. Mohammadi and D. Richon, *Chem. Eng. Sci.*, **66**, 2959 (2011).

28. F. Gharagheizi, A. Eslamimanesh, M. Sattari, A. H. Mohammadi and D. Richon, *AIChE J.*, **59**, 613 (2013).
29. F. Gharagheizi, A. Eslamimanesh, B. Tirandazi, A. H. Mohammadi and D. Richon, *Chem. Eng. Sci.*, **66**, 4991 (2011).
30. F. Gharagheizi, P. Ilani-Kashkouli and A. H. Mohammadi, *Chem. Eng. Sci.*, **78**, 204 (2012).
31. A. Golbraikh and A. Tropsha, *J. Mol. Graphics Modelling*, **20**, 269 (2002).
32. K. Golzar, S. Amjad-Iranagh and H. Modarress, *Ind. Eng. Chem. Res.*, **53**, 7247 (2014).
33. K. R. Harris, M. Kanakubo and L. A. Woolf, *J. Chem. Eng. Data*, **51**, 1161 (2006).
34. M. Hashemkhani, R. Soleimani, H. Fazeli, M. Lee, A. Bahadori and M. Tavalaeian, *J. Mol. Liq.*, **211**, 534 (2015).
35. S. Haykin, Neural networks: A comprehensive foundation: Macmillan college publishing company, New York (1994).
36. X. He, X. Zhang, S. Zhang, J. Liu and C. Li, *Fluid Phase Equilib.*, **238**, 52 (2005).
37. J. Hekayati and S. Raeissi, *J. Mol. Liq.*, **231**, 451 (2017).
38. A. Z. Hezave, M. Lashkarbolooki and S. Raeissi, *Fluid Phase Equilib.*, **352**, 34 (2013).
39. A. Z. Hezave, M. Lashkarbolooki and S. Raeissi, *Fluid Phase Equilib.*, **314**, 128 (2012).
40. A. Z. Hezave, S. Raeissi and M. Lashkarbolooki, *Ind. Eng. Chem. Res.*, **51**, 9886 (2012).
41. H. Jiang, Y. Zhao, J. Wang, F. Zhao, R. Liu and Y. Hu, *J. Chem. Thermodynam.*, **64**, 1 (2013).
42. G. W. Kauffman and P. C. Jurs, *J. Chem. Information Computer Sci.*, **41**, 408 (2001).
43. A. Kazakov, J. Magee, R. Chirico, V. Diky, C. Muzny, K. Kroenlein and M. Frenkel, Nist standard reference database 147: Nist ionic liquids database—(ilthermo), version 2.0, national institute of standards and technology, gaithersburg md, 20899.
44. F. Kermanpour and H. Niakan, *J. Chem. Thermodynam.*, **48**, 129 (2012).
45. M. Lashkarblooki, A. Z. Hezave, A. M. Al-Ajmi and S. Ayatollahi, *Fluid Phase Equilib.*, **326**, 15 (2012).
46. M. Lashkarbolooki, *Sep. Sci. Technol.*, **52**, 1454 (2017).
47. M. Lashkarbolooki, A. Z. Hezave and S. Ayatollahi, *Fluid Phase Equilib.*, **324**, 102 (2012).
48. M. Lashkarbolooki, A. Z. Hezave and A. Babapoor, *Korean J. Chem. Eng.*, **30**, 213 (2013).
49. M. Lashkarbolooki, Z. S. Shafipour and A. Z. Hezave, *J. Supercrit. Fluids*, **73**, 108 (2013).
50. M. Lashkarbolooki, Z. S. Shafipour, A. Z. Hezave and H. Farmani, *J. Supercrit. Fluids*, **75**, 144 (2013).
51. M. Lashkarbolooki, B. Vaferi, A. Shariati and A. Z. Hezave, *Fluid Phase Equilib.*, **343**, 24 (2013).
52. S. Laugier and D. Richon, *Fluid Phase Equilib.*, **210**, 247 (2003).
53. J. A. Lazzús, *J. Taiwan Inst. Chem. Engineers*, **40**, 213 (2009).
54. P. J. Linstrom and W. Mallard, Nist Chemistry Webbook; nist standard reference database no. 69 (2001).
55. H. Machida, R. Taguchi, Y. Sato, J. Smith and L. Richard, *J. Chem. Eng. Data*, **56**, 923 (2010).
56. S. Makridakis, S. C. Wheelwright and R. J. Hyndman, *Forecasting methods and applications*, John Wiley & Sons (2008).
57. S. G. Makridakis and S. C. Wheelwright, Forecasting methods for management (1989).
58. P. Mehra and B. W. Wah, *Artificial neural networks: Concepts and theory*, IEEE Computer Society Press Los Alamitos (1992).
59. G. Meindersma, M. Maase and A. De Haan, *Ionic liquids. Ullmann's encyclopedia of industrial chemistry*, Weinham: Wiley-VCH Verlag GmbH & Co. KGaA (2000).
60. Y. Miao, Q. Gan and D. Rooney, Artificial neural network model to predict compositional viscosity over a broad range of temperatures, *Intelligent Systems and Knowledge Engineering (ISKE), 2010 International Conference on*, IEEE, 668 (2010).
61. M. Mirarab, M. Sharifi, M. A. Ghayyem and F. Mirarab, *Fluid Phase Equilib.*, **371**, 6 (2014).
62. S. Mohanty, *Int. J. Refrigeration*, **29**, 243 (2006).
63. A. Mohebbi, M. Taheri and A. Soltani, *Int. J. Refrigeration*, **31**, 1317 (2008).
64. F. Nami and F. Deyhimi, *J. Chem. Thermodynam.*, **43**, 22 (2011).
65. H. Okuyucu, A. Kurt and E. Arcaklioglu, *Mater. Design*, **28**, 78 (2007).
66. M. Oliveira, M. Domínguez-Pérez, M. Freire, F. Llovell, O. Cabeza, J. Lopes-da-Silva, L. Vega and J. Coutinho, *J. Phys. Chem. B*, **116**, 12133 (2012).
67. M. S. Ozerdem, *J. Mater. Process. Technol.*, **208**, 470 (2008).
68. B. E. Poling, J. M. Prausnitz and J. P. O'connell, *The properties of gases and liquids*, Mcgraw-hill New York (2001).
69. P. Pratim Roy, S. Paul, I. Mitra and K. Roy, *Molecules*, **14**, 1660 (2009).
70. E. Rilo, M. Domínguez-Pérez, J. Vila, L. Varela and O. Cabeza, *J. Chem. Thermodynam.*, **49**, 165 (2012).
71. E. Rilo, J. Pico, S. García-Garabal, L. Varela and O. Cabeza, *Fluid Phase Equilib.*, **285**, 83 (2009).
72. A. A. Rohani, G. Pazuki, H. A. Najafabadi, S. Seyfi and M. Vossoughi, *Expert Systems with Applications*, **38**, 1738 (2011).
73. T. Ross, *J. Appl. Bacteriol.*, **81**, 501 (1996).
74. M. Sadrzadeh, T. Mohammadi, J. Ivakpour and N. Kasiri, *Chem. Eng. Process.: Process Intensification*, **48**, 1371 (2009).
75. M. Sadrzadeh, T. Mohammadi, J. Ivakpour and N. Kasiri, *Chem. Eng. J.*, **144**, 431 (2008).
76. M. Safamirzaei and H. Modarress, *Fluid Phase Equilib.*, **332**, 165 (2012).
77. M. Safamirzaei and H. Modarress, *Thermochim. Acta*, **545**, 125 (2012).
78. M. A. Sedghamiz, A. Rasoolzadeh and M. R. Rahimpour, *J. CO2 Utilization*, **9**, 39 (2015).
79. S. Seki, S. Tsuzuki, K. Hayamizu, Y. Umebayashi, N. Serizawa, K. Takei and H. Miyashiro, *J. Chem. Eng. Data*, **57**, 2211 (2012).
80. A. Shafiei, M. A. Ahmadi, S. H. Zaheri, A. Baghban, A. Amirfakhrian and R. Soleimani, *J. Supercrit. Fluids*, **95**, 525 (2014).
81. R. Soleimani, A. H. Saeedi Dehaghani and A. Bahadori, *J. Mol. Liq.*, **242**, 701 (2017).
82. Z. Sterjovski, D. Nolan, K. Carpenter, D. Dunne and J. Norrish, *J. Mater. Process. Technol.*, **170**, 536 (2005).
83. M. Tariq, M. G. Freire, B. Saramago, J. A. Coutinho, J. N. C. Lopes and L. P. N. Rebelo, *Chem. Soc. Rev.*, **41**, 829 (2012).
84. J. Taskinen and J. Yliruusi, *Adv. Drug Delivery Rev.*, **55**, 1163 (2003).
85. J. S. Torrecilla, J. Palomar, J. García, E. Rojo and F. Rodríguez, *Che-*

mometrics Intelligent Laboratory Systems, **93**, 149 (2008).
86. J. S. Torrecilla, F. Rodríguez, J. L. Bravo, G. Rothenberg, K. R. Seddon and I. López-Martin, *Phys. Chem. Chem. Phys.*, **10**, 5826 (2008).
87. J. Troncoso, C. A. Cerdeiriña, Y. A. Sanmamed, L. Romaní and L. P. N. Rebelo, *J. Chem. Eng. Data*, **51**, 1856 (2006).
88. S. Urata, A. Takada, J. Murata, T. Hiaki and A. Sekiya, *Fluid Phase Equilib.*, **199**, 63 (2002).
89. G. Vakili-Nezhaad, M. Vatani, M. Asghari and I. Ashour, *J. Chem. Thermodynam.*, **54**, 148 (2012).
90. L. F. Vega, O. Vilaseca, F. Llovell and J. S. Andreu, *Fluid Phase Equilib.*, **294**, 15 (2010).
91. A. Wandschneider, J. K. Lehmann and A. Heintz, *J. Chem. Eng. Data*, **53**, 596 (2008).
92. J.-y. Wang, H.-c. Jiang, Y.-m. Liu and Y.-q. Hu, *J. Chem. Thermodynam.*, **43**, 800 (2011).
93. J.-Y. Wang, F.-Y. Zhao, Y.-M. Liu, X.-L. Wang and Y.-Q. Hu, *Fluid Phase Equilib.*, **305**, 114 (2011).
94. Y. Wei, Q.-G. Zhang, Y. Liu, X. Li, S. Lian and Z. Kang, *J. Chem. Eng. Data*, **55**, 2616 (2010).
95. I. H. Witten, E. Frank, M. A. Hall and C. J. Pal, *Data mining: Practical machine learning tools and techniques*, Morgan Kaufmann (2016).
96. J. Zupan and J. Gasteiger, *Neural networks for chemists: An introduction*, John Wiley & Sons, Inc. (1993).